Electronic structure of $La_{0.7}Sr_{0.3}Mn_{1-x}Cu_xO_3$ ($0.0 \leq x \leq 0.30$)

2008 J. Phys.: Condens. Matter 20 255228

(http://iopscience.iop.org/0953-8984/20/25/255228)

J. Phys.: Condens. Matter **20** (2008) 255228 (7pp) doi:10.1088/0953-8984/20/25/255228

Electronic structure of $La_{0.7}Sr_{0.3}Mn_{1-x}Cu_xO_3$ ($0.0 \leqslant x \leqslant 0.30$)

M S Kim[1,2], J B Yang[1,2,4], J Medvedeva[1], W B Yelon[2,3], P E Parris[1] and W J James[2,3]

[1] Department of Physics, University of Missouri-Rolla, Rolla, MO 65409, USA
[2] Graduate Center for Materials Research, University of Missouri-Rolla, Rolla, MO 65409, USA
[3] Department of Chemistry, University of Missouri-Rolla, Rolla, MO 65409, USA

E-mail: jinbo@mst.edu

Received 26 February 2008
Published 22 May 2008
Online at stacks.iop.org/JPhysCM/20/255228

Abstract

We have investigated the electronic structure of Cu-substituted $La_{0.7}Sr_{0.3}MnO_3$ (LSMO) by x-ray photoelectron spectroscopy and using density functional theory within local spin-density approximations (LSDA) and LSDA + U. We find that there is a coexistence of mixed-valent Cu ions, Cu^{3+} with Cu^{2+} dominant, in all Cu-substituted LSMO samples. From a deconvolution of the XPS spectra of Cu-$2p_{3/2}$, we determined the ratios of Cu^{2+}/Cu^{3+} and Mn^{3+}/Mn^{4+}, and in turn calculated the change in the tolerance factors of Cu-substituted LSMO. Valence-band photoelectron spectra show that the density of states at the Fermi level is made up mainly of the O-2p and Mn-3d states with a small contribution near E_F from the Cu-3d states. We find that LSDA + U calculations for $La_{1/2}Sr_{1/2}Mn_{1-x}Cu_xO_3$ describe the half-metallicity and ground state ferromagnetic ordering with no evidence of antiferromagnetism for all systems consistent with experimental neutron diffraction data. Two electron transport channels of the major Mn–O–Mn and the minor Cu–O–Cu chains are found. This suggests that the electronic transport behavior of Cu-substituted LSMO systems may be explained by a combination of two different transport mechanisms: (i) a σpd hybridization between the e_g states in a majority spin-up Mn-d channel with O-2p orbitals in the Mn–O–Mn chain and (ii) a σpd hybridization between the e_g states in a dominant minority spin-down Cu-d channel with O-2p orbitals in the Cu–O–Cu chain. We also find that the half-metallicity of the compounds is lost upon Cu-substitution with a resulting anisotropic electronic transport of the Cu-pair electrons in the basal plane and along the c axis.

1. Introduction

The ABO_3 (A = trivalent rare earth atom, B = 3d transitional metal) perovskites have attracted considerable attention because of their anomalous magnetic and transport properties such as colossal magnetoresistance (CMR) and metal–insulator transitions (MIT). The $La_{1-x}Sr_xMnO_3$ perovskites are canonical ABO_3-type CMR materials. It has been reported that double-exchange (DE) interactions together with Jahn–Teller (JT) distortions in the MnO_6 octahedron may be responsible for the large MR effects [1–4]. Because the mixed-valent Mn ion is the center of the DE interaction, the role of the Mn atom and its local environment have become the focus of much of the research on manganese perovskites. To investigate the CMR associated with the lattice deformation and charge ordering of the crucial Mn–O–Mn network, many early studies were carried out by substitution of the A-site with divalent atoms (Ca, Sr, Ba, etc) [5–7]. It has also been shown that substitution of the Mn (B-site) by other atoms dramatically affects the magnetic and transport properties of manganese perovskites. The B-site modification directly affects the Mn network by changing the Mn^{3+}/Mn^{4+} ratio and the electron carrier density [8–11].

Previously, we have studied the structural, magnetic and transport properties of $La_{0.7}Sr_{0.3}Mn_{1-x}Cu_xO_3$ ($0 \leqslant x \leqslant 0.20$) using x-ray diffraction, neutron diffraction, magnetization and resistivity measurements. The changes in the lattice

[4] Author to whom any correspondence should be addressed.

Table 1. Refined lattice parameters, a, c and unit cell volume of $La_{0.7}Sr_{0.3}Mn_{1-x}Cu_xO_3$ ($0 \leqslant x \leqslant 0.30$) at room temperature (RT). Numbers in parentheses are statistical errors. O_{occ} is the site occupation number, m is the magnetic moment of the Mn site. d_{Mn-O} is the Mn–O bond length, $\theta_{Mn-O-Mn}$ is the Mn–O–Mn bond angle.

x	a (Å)	c (Å)	Volume (Å^3)	O_{occ}	m (μ_B)	d_{Mn-O} (Å)	$\theta_{Mn-O-Mn}$ (deg)
			$T = 300$ K				
0.00	5.5039(1)	13.3553(5)	350.365(18)	0.500	2.514	1.9537	166.351
0.05	5.5003(1)	13.3387(4)	349.474(17)	0.500	2.053	1.9517	166.515
0.10	5.5036(2)	13.3502(6)	350.191(22)	0.502	1.980	1.9507	166.733
0.15	5.4982(2)	13.3304(6)	348.985(21)	0.500	1.350	1.9504	166.701
0.20	5.4943(2)	13.3184(6)	348.178(24)	0.513	0.000	1.9492	165.576
			$T = 10$ K				
0.00	5.4811(1)	13.2756(3)	345.397(13)	0.500	3.442	1.9451	166.035
0.05	5.4843(1)	13.2795(4)	345.909(17)	0.498	3.299	1.9450	166.532
0.10	5.4822(1)	13.2734(4)	345.480(17)	0.502	3.279	1.9442	166.556
0.15	5.4857(2)	13.2715(4)	345.872(17)	0.500	2.215	1.9458	166.127
0.20	5.4855(2)	13.2636(4)	345.636(17)	0.513	0.895	1.9456	165.983

parameters obtained from neutron diffraction studies indicated the existence of mixed-valent Cu ions, Cu^{2+} and Cu^{3+} in this system [11].

In this paper, we present the results of an x-ray photoelectron spectroscopy (XPS) study on the core-level and valence-band photoelectron spectroscopy (PES) of $La_{0.7}Sr_{0.3}Mn_{1-x}Cu_xO_3$ ($0 \leqslant x \leqslant 0.30$). To investigate the origin of the XPS peaks and the detailed band structure of p–d hybridization between Mn–O–Mn and Cu–O–Cu channels, *ab initio* electronic band-structure calculations were performed for $La_{1/2}Sr_{1/2}MnO_3$ and a hypothetical $La_{1/2}Sr_{1/2}Mn_{1-x}Cu_xO_3$ ($x = 1/6, 1/3$) system. These studies provide further evidence for the existence of mixed-valent Cu ions and the effect of Cu–O–Cu percolation channels on the electronic transport properties.

2. Experimental details

Samples of $La_{0.7}Sr_{0.3}Mn_{1-x}Cu_xO_3$, $0 \leqslant x \leqslant 0.30$, were prepared using the conventional solid state reaction method. Detailed sample preparation and physical property measurements, such as x-ray diffraction, neutron diffraction (ND), saturation magnetization and resistivity measurements, are described in a previous study [11].

The spectra of core-level x-ray photoelectron spectroscopy (XPS) and valence-band photoelectron spectroscopy (PES) of the samples were obtained with monochromatic Al Kα radiation ($h\nu = 1496.6$ eV) using an AXIS 165 spectrometer. The energy spectra were analyzed with a hemispherical mirror analyzer having an energy resolution of 0.5 eV. The spectra were measured at an accelerating voltage of 15 kV and an output power of 225 W below 7×10^{-10} Torr.

The LSDA + U calculations were performed for $La_{1/2}Sr_{1/2}MnO_3$ and a hypothetical supercell of $La_{1/2}Sr_{1/2}Mn_{1-x}Cu_xO_3$ ($x = 1/6, 1/3$) in the framework of the tight-binding linearized muffin-tin orbital method in the atomic-sphere approximation (TB-LMTO-ASA) [12–14]. The crystal parameters of the parent compound, $La_{1/2}Sr_{1/2}MnO_3$, were taken from previous studies by Spooren *et al* [15]. In the case of $La_{1/2}Sr_{1/2}Mn_{1-x}Cu_xO_3$ ($x = 1/6, 1/3$), the same lattice parameters and atomic positions for $La_{1/2}Sr_{1/2}MnO_3$ were used. Based on a previous study [11] of Cu-substituted LSMO, it was assumed that the structural parameters were nearly equal and do not produce any significant change in the band structure of the hypothetical structure. For the LSDA + U calculations, values of the Coulomb and exchange parameters $U = 7$ eV and $J = 0.79$ eV were taken from the studies of Medvedeva *et al* [16]. The von Barth–Heidin–Janak local exchange–correlation potential was used [17]. The self-consistent convergence criterion of total energy is 10^{-4} eV and the charge density is 1.0×10^{-6}/unit cell.

3. Results and discussion

Table 1 presents the structural information of Cu-substituted LSMO, with $0 \leqslant x \leqslant 0.30$, obtained from ND measurements at RT and 10 K and Rietveld refinements [11]. The $R\bar{3}c$ rhombohedral space-group was used to fit the crystal structure and the $P1$ group was used to fit the magnetic structure. The lattice parameters a and c decrease only slightly with increasing Cu content at RT, but at $T = 10$ K the lattice parameters remain almost constant with increasing Cu content.

Tolerance factors were calculated to examine the stability and strains of these systems. The tolerance factor τ is given by the formula: $\tau = (r_{(La,Sr)} + r_O)/[(r_{(Mn,Cu)} + r_O)\sqrt{2}]$, where $r_{(La,Sr)}$, $r_{(Mn,Cu)}$ and r_O are the average radii of the A-sites, B-sites and oxygen, respectively. The B-site (six-coordinated) ionic radius of Cu^{2+} (0.73 Å) is larger than Mn^{3+} (Mn^{4+}) and the ionic radius of Cu^{3+} (0.54 Å) is close to that of Mn^{4+} (0.53 Å) and smaller than the radius of the high spin state of Mn^{3+} (0.645 Å) [18]. If Cu^{3+} only exists and replaces Mn^{3+}, the tolerance factor increases from 0.979 ($x = 0.0$) to 0.989 ($x = 0.30$), $\Delta\tau > 1\%$, which means that the lattice parameters decrease linearly. If Cu^{2+} ions replace Mn^{3+} (or Mn^{4+}), the tolerance factor decreases and the lattice parameters increase. Therefore, if the value of τ is between the above two ranges, the change of lattice parameters depends on which ionic state of Cu is dominant and to what extent it changes the Mn^{3+}/Mn^{4+} ratio under the constraint of charge balance. Considering the coexistence of Cu^{2+} and

Table 2. Fitting parameters of the Mn $2p_{3/2}$ XPS spectrum of $La_{0.7}Sr_{0.3}Mn_{1-x}Cu_xO_3$ ($0 \leqslant x \leqslant 0.30$). ΔE is the separation of binding energies between two neighboring fitting components. I_i denotes the fractional intensity of the ith component as calculated by integrating the fitting areas.

	Binding energy (eV)			ΔE (eV)		Intensity		
x	C1	C2	C3	C2 − C1	C3 − C2	I_1/I	I_2/I	I_3/I
0.00	640.5145	641.6036	643.2231	1.0895	1.6195	0.1314	0.5768	0.2918
0.05	640.4701	641.5971	643.1154	1.1270	1.5183	0.2009	0.4499	0.3492
0.15	640.4694	641.5180	643.2786	1.0505	1.2749	0.3286	0.3749	0.2965
0.20	640.5682	641.6924	642.5445	1.1242	0.8521	0.1461	0.3827	0.4711
0.25	640.4436	641.5121	642.9584	1.0685	1.4463	0.0852	0.5106	0.4042
0.30	640.5580	641.6085	642.8834	1.0486	1.7606	0.1180	0.5992	0.2829

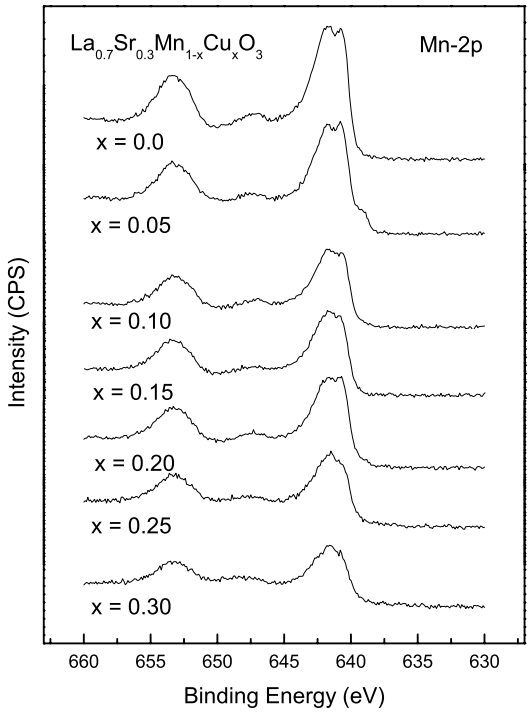

Figure 1. Mn-2p XPS of $La_{0.7}Sr_{0.3}Mn_{1-x}Cu_xO_3$ ($0 \leqslant x \leqslant 0.30$) at room temperature.

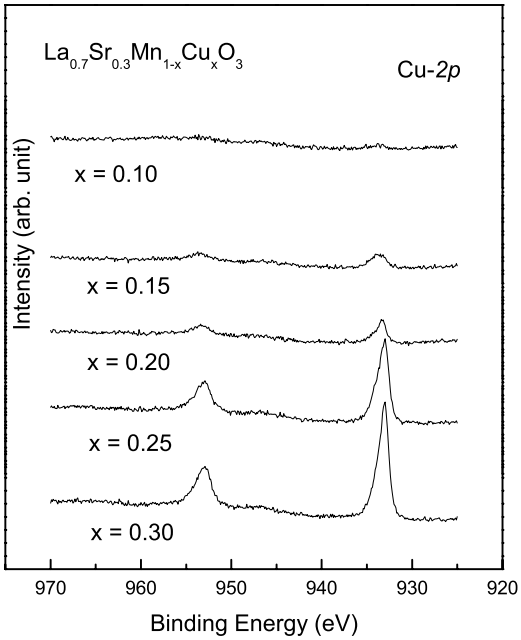

Figure 2. Cu-2p XPS of $La_{0.7}Sr_{0.3}Mn_{1-x}Cu_xO_3$ ($0.05 \leqslant x \leqslant 0.30$) at room temperature.

Cu^{3+}, the tolerance factor increases only slightly ($\Delta\tau < 0.6\%$) and the lattice parameters decrease slightly with increasing Cu content. These results agree well with the experimental results and suggest that Cu^{2+} and Cu^{3+} coexist with the dominant Cu^{2+} state [11]. Thus, the changes in the lattice parameters, (Mn,Cu)–O bond length and (Mn,Cu)–O–(Mn,Cu) bond angle at RT and low temperature may be ascribed to a mixed state of Cu^{2+}/Cu^{3+}.

X-ray photoelectron spectrometer (XPS) measurements were then initiated to investigate the core-level and valence band of the Mn and Cu ions. The Mn-2p spectra, figure 1, consist of three peaks located at ∼641, 653 and 647 eV for the spin–orbit doublet Mn $2p_{3/2}$, Mn $2p_{1/2}$ and a satellite structure, respectively. The intensity of the two main peaks decreases and becomes broad with increasing Cu content. The satellite peak, which arises from the mixed state of Mn^{3+} and Mn^{4+}, shifts to the high binding-energy (BE) region with increasing Cu content likely due to the increase of Mn^{4+}. To deconvolute the spectra so as to calculate the Mn $2p_{3/2}$ spectrum, two main components were used with one extra component whose BEs were 640.5, 641.6 and 643.0 eV, respectively, table 2. In fitting the Mn $2p_{3/2}$ spectra, the existence of two different initial states of Mn^{3+} and Mn^{4+} was unlikely to be the origin of the two main components because the Mn-2p core levels of Mn^{3+} and Mn^{4+} ions have very similar band structures. The energy separation between them is $\Delta_{ex} \sim 1.1$ eV and is not changed with increasing Cu content. This is about the same order of magnitude as the exchange interaction between core holes and the valence electrons, about 1.3 eV [19]. The relative intensity I_1/I, the ratio of the first component area to the total area of the $2p_{3/2}$ spectrum, increases up to $x = 0.15$ and decreases with further Cu substitution. In contrast, the relative intensity I_2/I, the ratio of the second component area to the total area of the $2p_{3/2}$ spectrum, decreases up to $x = 0.15$ and then increases with further Cu substitution.

The Cu-2p spectra, figure 2, consist of two peaks located at 933 and 953 eV for Cu $2p_{3/2}$ and $2p_{1/2}$, respectively. A broad satellite peak is located around 946 eV. The Cu-2p peaks

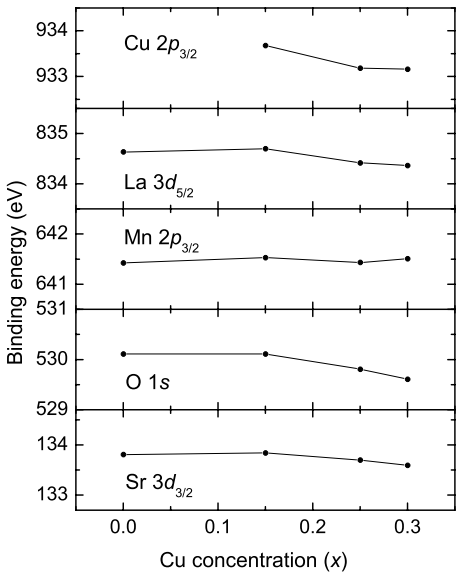

Figure 3. Binding-energy shift of core levels in $La_{0.7}Sr_{0.3}Mn_{1-x}Cu_xO_3$ ($0 \leqslant x \leqslant 0.30$) at room temperature. For the La-3d$_{5/2}$ peak, the lower binding-energy peak is listed.

Table 3. Fitting parameters of the Cu 2p$_{3/2}$ XPS spectrum of $La_{0.7}Sr_{0.3}Mn_{1-x}Cu_xO_3$ ($0 \leqslant x \leqslant 0.30$). ΔE is the separation of binding energies between two neighboring fitting components. I_i denotes the fractional intensity of the ith component as calculated by integrating the fitting areas.

	Binding energy (eV)			Intensity	
x	C1 (Cu^{2+})	C2 (Cu^{3+})	ΔE (eV)	I_1/I	I_2/I
0.15	933.5181	934.4725	0.9544	0.8800	0.1200
0.20	933.3079	934.2931	0.9852	0.8000	0.2000
0.25	933.0281	934.0556	1.0275	0.7850	0.2150
0.30	932.7809	933.7378	0.9569	0.6770	0.3230

shift to the lower BE side with increasing Cu content. The Cu 2p$_{3/2}$ spectrum was deconvoluted with two components corresponding to the Cu^{2+} and the Cu^{3+} states [19, 20]. Table 3 presents the fitting parameters of the Cu 2p$_{3/2}$ spectra of $La_{0.7}Sr_{0.3}Mn_{1-x}Cu_xO_3$ ($0 \leqslant x \leqslant 0.30$). The dominant Cu^{2+} state decreases linearly with increasing Cu content, while the minority Cu^{3+} state increases with increasing Cu content. The separation of BE between Cu^{2+} and Cu^{3+}, $\Delta E \sim 1.0$ eV, is not changed with increasing Cu content. The BEs of both Cu^{2+} and Cu^{3+} states shift to the lower BE region which suggests that the Cu-2p state may be strongly hybridized with the O-1s state.

Figure 3 presents the BE shift of core levels as a function of Cu content. The BEs of all the core levels shift to the lower BE region, which suggests that the E_F is lowered by introducing holes with Cu substitution. This is very similar to the hole doping effects on the A-site in $La_{1-x}Sr_xMnO_3$ [21].

From the results of a deconvolution of the Cu-2p peak we can estimate the ratio of Cu^{2+}/Cu^{3+} and in turn the fractional ratio of Mn^{3+}/Mn^{4+}. Considering the parent compound LSMO, the cation distributions at the A- and B-sites indicate the Mn atom to be in mixed valence states,

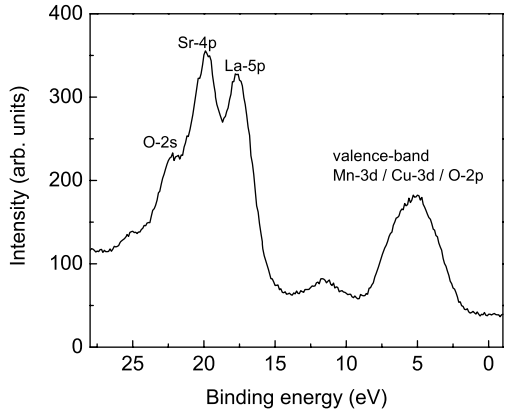

Figure 4. Experimental valence-band XPS spectra of $La_{0.7}Sr_{0.3}Mn_{0.85}Cu_{0.15}O_3$.

Table 4. Evolution of the ionic content of the Mn site and the tolerance factors (τ) of $La_{0.7}Sr_{0.3}Mn_{1-x}Cu_xO_3$ ($0 \leqslant x \leqslant 0.30$).

	Mole content of B(Mn, Cu)-site					
x	Cu^{2+}	Cu^{3+}	Mn^{3+}	Mn^{4+}	Mn^{3+}/Mn^{4+}	τ
0.00	0.000	0.000	0.700	0.300	2.3333	0.979
0.15	0.132	0.018	0.418	0.432	0.9676	0.982
0.20	0.160	0.040	0.340	0.460	0.7391	0.984
0.25	0.196	0.054	0.254	0.496	0.5113	0.985
0.30	0.204	0.096	0.196	0.504	0.3889	0.987

$(La^{3+}_{0.7}Sr^{2+}_{0.3})_A(Mn^{3+}_{0.7}Mn^{4+}_{0.3})_BO^{2-}_3$. From the ND analysis, we confirmed that the Cu goes to the Mn site. In addition, we assume that the La, Sr and O starting stoichiometry holds and does not induce any charge valence fluctuations at the Mn site. Then, it is necessary that the ratio of Cu^{2+}/Cu^{3+} and Mn^{3+}/Mn^{4+} satisfy charge balance and charge neutrality in these compounds. Accordingly, the full ionic configuration of x moles of Cu-substituted LSMO can be represented by

$$(La^{3+}_{0.7}Sr^{2+}_{0.3})_{A-site}\Big((Cu^{2+}_{(1-\alpha)}Cu^{3+}_{\alpha})_x \Big(Mn^{3+}_{(0.7+\frac{\alpha-1.3}{1-x}x)}Mn^{4+}_{(0.3-\frac{\alpha-1.3}{1-x}x)}\Big)_{1-x}\Big)_{B-site}O^{2-}_3, \quad (1)$$

where x is the mole percent of Cu on the B-site and α is the ratio of Cu^{3+} to total Cu content. The value of 1.3 varies with the hole substitution ratio and charge valence of the substituted ion. Table 4 presents the evolution of the Mn-site ionic content and the calculated tolerance factors based on the determined ionic content. For instance, for $x = 0.15$, the Cu^{3+} content as determined from XPS measurements is 1.8 mol% at the Mn site and the Mn^{3+}/Mn^{4+} ratio is calculated to be 0.967. For $x = 0.25$, the Cu^{3+} content increases to 5.4 mol% at the Mn site and the Mn^{3+}/Mn^{4+} ratio is calculated to be 0.5113. The per cent ratio of Cu^{3+} to total Cu content gradually increases, while the per cent ratio of Mn^{3+} to total Mn content dramatically decreases. The change of the tolerance factor, from LSMO ($x = 0$–0.30), is $\Delta\tau \sim 0.82\%$, which means that the lattice parameters increase slightly. This agrees well with the ND data.

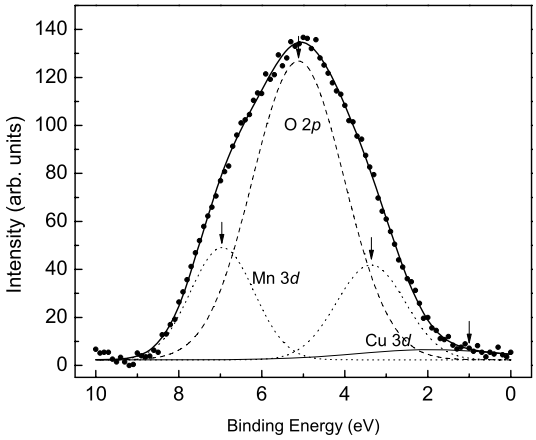

Figure 5. Calculated (solid line) and experimental (dots) x-ray photoelectron spectra for the valence band of $La_{0.7}Sr_{0.3}Mn_{0.85}Cu_{0.15}O_3$.

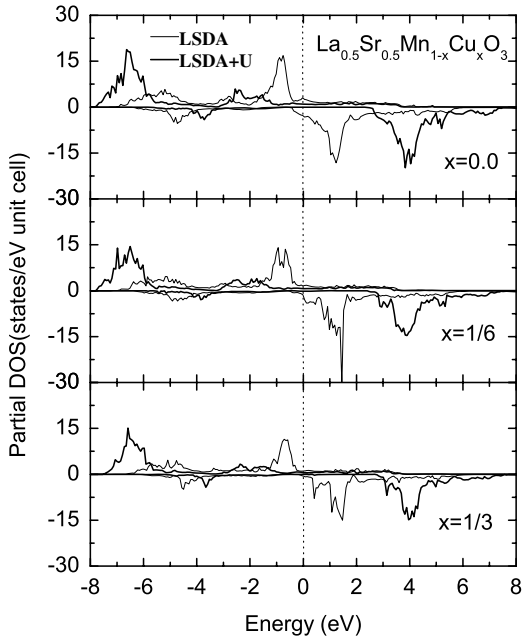

Figure 6. Total density of states (DOS) of the Mn-d states of ferromagnetic $La_{0.5}Sr_{0.5}Mn_{1-x}Cu_xO_3$ ground state from LSDA (solid line) and LSDA + U with $U = 7$ eV (thick solid line) calculations. The minority-spin contributions are shown as negative values. The Fermi level is set to 0 eV.

Figure 4 shows the valence-band spectrum of $La_{0.7}Sr_{0.3}Mn_{0.85}Cu_{0.15}O_3$. Three peaks are found at 17.61, 19.89 and 22.23 eV which can be attributed to the La-5p, Sr-4p and O-2s states, respectively [21, 22]. A satellite peak is observed at about 11.61 eV which may be of the Mn–O dsp hybrid character. The PES spectra were calculated based on the results of the partial density of states of $La_{1/2}Sr_{1/2}Mn_{5/6}Cu_{1/6}O_3$, figure 5. The calculated peak positions and the width fit well with the experimental spectra. The peak position of the O-2p component, ∼5 eV, agrees well with the peak in the ultraviolet photoemission (UPS) spectra [23]. Five prominent peaks are determined at 3.4, 7.0 eV for Mn-3d, at 5.1 eV for the O-2p state, and at 1.9 eV for the Cu-3d states. According to the

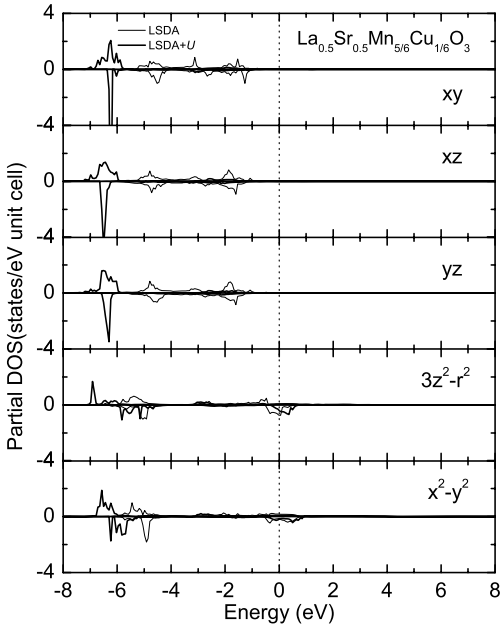

Figure 7. Partial density of states (PDOS) of the Cu-d states of the ferromagnetic $La_{0.5}Sr_{0.5}Mn_{5/6}Cu_{1/6}O_3$ ground state from LSDA (solid line) and LSDA + U with $U = 7$ eV (thick solid line) calculations. The minority-spin contributions are shown as negative values. The Fermi level is set to 0 eV.

photoionization cross section for $La_{1-x}Sr_xMnO_3$, the emission intensity is mostly due to the O-2p, and the Mn-3d state accounts for about 30% of the total valence-band intensity [24]. From the area integration of calculated curves, the ratio of the contribution to the total valence-band intensity, O-2p:Mn-3d:Cu-3d, is 64.3:32.7:3.1.

To see the Cu effect on the properties of LSMO compounds, the electronic structures of a supercell of $La_{1/2}Sr_{1/2}MnO_3$ and the hypothetical Cu-substituted $La_{1/2}Sr_{1/2}Mn_{1-x}Cu_xO_3$, $x = 1/6, 1/3$, were calculated using the LSDA + U method. Each supercell $La_3Sr_3Mn_6O_{18}$ has six $LaMnO_3$ formula units. Initially, the total energy was calculated for different atomic arrangements to determine the most energetically favorable configuration. Then, band-structure calculations were done both for the ferromagnetic (FM) and for the A-type antiferromagnetic (AFM) phases of the above compounds.

The LSDA + U results give a strong FM interaction without any sign of antiferromagnetism for all three systems, which is consistent with experimental ND data [15]. When compared with previous work [16], no significant changes are observed for the Mn-d states with increasing Cu content and only e_g states in the majority-spin channel contribute to the DOS at E_F, figure 6. (LSDA calculations are shown for comparative purposes.)

Figures 7 and 8 show the partial DOS of Cu-d states for $x = 1/6, 1/3$, respectively. As seen from the figures, only the e_g states ($x^2 - y^2$ and $3z^2 - r^2$ orbitals) in the d-band contribute to the DOS at E_F. The t_{2g} bands (xy and the degenerate xz and yz) are located about 6.3 eV below E_F and the DOS become weaker and more delocalized with increasing Cu content. When Cu is introduced, the half-metallicity disappears. This

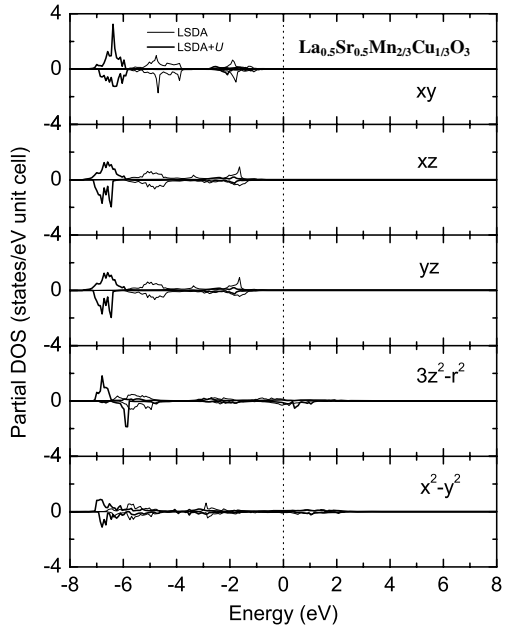

Figure 8. Partial density of states (PDOS) of the Cu-d states of ferromagnetic $La_{0.5}Sr_{0.5}Mn_{2/3}Cu_{1/3}O_3$ ground state from LSDA (solid line) and LSDA + U with $U = 7$ eV (thick solid line) calculations. The minority-spin contributions are shown as negative values. The Fermi level is set to 0 eV.

is mainly due to the strong hybridization between the spin-down Cu-d state and neighboring O-2p orbitals, which induces a redistribution of the charge density of Mn atoms. Only the d-states of the Cu e_g orbitals and the p-states of the neighboring oxygen contribute to the minority DOS at the Fermi level.

The LSDA + U model provides a good description of the spin-dependent electronic properties. Table 5 presents the LSDA + U calculations for $La_{1/2}Sr_{1/2}Mn_{1-x}Cu_xO_3$, $x = 0, 1/6, 1/3$. The contribution of the majority-spin channel to the DOS at the Fermi level, $N^{\uparrow}(E_F)$, does not change with increasing Cu content; 2.7, 2.8, 2.7 states for $x = 0, 1/6, 1/3$, respectively. However, the contribution of the minority-spin channel to the DOS at the Fermi level, $N^{\downarrow}(E_F)$, changes with increasing Cu content; 0 (half-metallic), 1.9, 1.6 states eV^{-1} for $x = 0, 1/6, 1/3$, respectively.

To investigate the anisotropy of the electronic conduction of Mn and Cu atoms at E_F, the ratios between the e_g states of $x^2 - y^2$ and $3z^2 - r^2$ contributing to the DOS (E_F) were calculated. For the Mn atom, we have an almost isotropic electronic transport character with a ratio of ∼1 for all three samples. However for Cu atoms, the contribution from the $3z^2 - r^2$ orbital is about three times larger than that from the $x^2 - y^2$ orbital and the ratio is not changed with increasing Cu content. The anisotropic character of Cu transport suggests that electron hopping along the c axis is preferable to that in the Cu–O chains in the ab plane.

The effective exchange interaction parameters were calculated to determined the effect of Cu substitution on the exchange coupling of Mn atoms. The exchange interaction parameters J_{dd}^{ab} between Mn pairs located close to the Cu ion decrease with increasing Cu content, while the parameter J_{dd}^{c} between Mn pairs located further away from Cu slightly

Table 5. The calculated parameters of LDA + U ($U = 7$ eV) of $La_{0.7}Sr_{0.3}Mn_{1-x}Cu_xO_3$ ($x = 0, 1/6, 1/3$). The contribution of the up-spins and down-spins to the DOS at E_F, $N^{\uparrow}(E_F)$ and $N^{\downarrow}(E_F)$, respectively; the ratio of the $3z^2 - r^2$ and $x^2 - y^2$ orbital contribution to the DOS at E_F; m (μ_B) is a magnetic moment of each atom; effective d–d exchange parameters between neighboring Mn atoms, J_{dd}^{ab} in the ab plane and J_{dd}^{c} (eV) along the c axis; Curie temperature T_C (K).

LDA + U	$x = 0$	$x = 1/6$	$x = 1/3$
$N^{\uparrow}$ (E_F) (States/eV unit cell)	2.7	2.8	2.7
$N^{\downarrow}$ (E_F) (States/eV unit cell)	0.0	1.9	1.6
$N^{\uparrow}_{3z^2-r^2}$ (Mn)/$N^{\uparrow}_{x^2-y^2}$ (Mn)	1.05	1.09	1.30
$N^{\downarrow}_{3z^2-r^2}$ (Cu)/$N^{\downarrow}_{x^2-y^2}$ (Cu)	—	2.77	2.81
m (μ_B)/Mn	3.61	3.60	3.57
m (μ_B)/Cu	—	0.225	0.069
J_{dd}^{ab} (meV)	43.3	42.0	36.4
J_{dd}^{c} (meV)	44.7	45.9	47.5
T_C (K)	481	383	265

increase with increasing Cu content. At any rate, there is no antiferromagnetic coupling induced by Cu. These results agree with the ND data and saturation magnetization measurements. The slight suppression of J_{dd}^{ab} can be explained by the fact that the Mn and Cu share a neighboring oxygen.

The average magnetic moment on the Mn atoms slightly decreases from 3.614, 3.593, 3.571 μ_B/Mn for $x = 0, 1/6, 1/3$, respectively. For the Cu ions, small magnetic moments are obtained with 0.225, 0.069 μ_B/Cu for $x = 1/6, 1/3$, respectively. Using the calculated exchange parameters, we estimate the Curie temperature within the mean-field approximation as

$$T_C = \frac{2S_i(S_i + 1)}{3k_B} \sum_{\alpha}^{n} z_{i\alpha} J_{i\alpha}, \qquad (2)$$

where S_i is the spin of the ith ion and $J_{i\alpha}$ is the exchange integral between the ith and αth ions. We also assume that the dilution of Mn moments affects $z_{i\alpha}$ in a linear fashion, $z_{i\alpha}(n_p) \propto (1 - n_p) z_{i\alpha}(0)$, where $z_{i\alpha}(0)$ refers to the undiluted system and n_p is a relative substitutional concentration. The estimated T_C is 481 K, 383 K and 265 K for $x = 0, 1/6, 1/3$, respectively. Again the calculated T_Cs are higher in value than those of the real systems due to the larger magnetic moments.

4. Summary

In summary, we have investigated the electronic structure of Cu-substituted $La_{0.7}Sr_{0.3}Mn_{1-x}Cu_xO_3$ by XPS, PES and *ab initio* density functional LSDA and LSDA+U calculations. Mixed-valent Cu ions, Cu^{3+} with dominant Cu^{2+}, are observed in all of the Cu-substituted LSMOs. LSDA + U calculations reveal that the electronic transport behavior is well described by a combination of two different conduction mechanisms resulting from (i) pd hybridization of the $e_g^{\uparrow}$ states in the majority spin-Mn-3d channel with O-2p orbitals in the Mn–O–Mn chain and (ii) pd hybridization of $e_g^{\downarrow}$ states in the minority spin-Cu-3d channel with O-2p orbitals in the Cu–O–Cu chain. We also find that the half-metallicity of compounds is lost upon Cu substitution. The contribution from the $3z^2 - r^2$ orbital is

about three times larger than the x^2-y^2 orbital, which indicates anisotropic electronic transport resulting from the Cu states.

Acknowledgments

The authors thank Jeff Wight for invaluable help in the XPS measurements. The support by DOE under contract DOE/BES grant DE-FG02-05ER46245 is acknowledged.

References

[1] Zener C 1951 *Phys. Rev.* **82** 403
[2] Goodenough J B 1963 *Magnetism and the Chemical Bond* (New York: Interscience)
[3] Kubo K and Ohata N 1972 *J. Phys. Soc. Japan* **33** 21
[4] Millis A J, Littlewood P B and Shraiman B I 1995 *Phys. Rev. Lett.* **74** 5144
[5] von Helmolt R, Wecker J, Holzapfel B, Schultz L and Samwer K 1993 *Phys. Rev. Lett.* **71** 2331
[6] Neumeier J J, Andres K and McClellan K J 1999 *Phys. Rev.* B **59** 1701
[7] Medarde M, Mesot J, Lacorre P, Rosenkranz S, Fischer P and Gobrecht K 1995 *Phys. Rev.* B **52** 9248
[8] Martin C, Maignan A and Raveau B 1996 *J. Mater. Chem.* **6** 1245
[9] Blasco J, Garcia J, de Teresa J M, Ibarra M R, Perez J, Algarabel P A, Marquina C and Ritter C 1997 *Phys. Rev.* B **55** 8905
[10] Kim M S, Yang J B, Cai Q, Zhou X D, James W J, Yelon W B, Parris P E, Buddhikot D and Malik S K 2005 *Phys. Rev.* B **71** 014433
[11] Kim M S, Yang J B, Cai Q, Zhou X D, James W J, Yelon W B, Parris P E, Buddhikot D and Malik S K 2005 *J. Appl. Phys.* **97** 10H714
[12] Andersen O K and Jepsen O 1984 *Phys. Rev. Lett.* **53** 2571
[13] Gunnarsson O, Andersen O K, Jepsen O and Zaanen J 1989 *Phys. Rev.* B **39** 1708
[14] Anisimov V I and Gunnarsson O 1991 *Phys. Rev.* B **43** 7570
[15] Spooren J, Walton R I and Millange F 2005 *J. Mater. Chem.* **10** 1039
[16] Medvedeva J E, Anisimov V I, Mryasov O N and Freeman A J 2002 *J. Phys.: Condens. Matter* **14** 4533
[17] Janak J F 1975 *Phys. Rev.* B **12** 1257
[18] Shannon R D 1976 *Acta Crystallogr.* A **32** 751
[19] Huang D J, Riffe D M and Erskine J L 1995 *Phys. Rev.* B **51** 15170
[20] Steiner P, Hafner S, Kinsinger V, Sander I, Siegwatt B, Schmitt H, Schultz R, Junk S, Schwitzgebel G, Gold A, Politis C, Miller H P, Hoppe R, Kemmlei S and Kunz C 1988 *Z. Phys.* B **69** 449
[21] Saitoh T, Bocquet A E, Mizokawa T, Namatame H, Fujimori A, Abbate M, Takeda Y and Takano M 1995 *Phys. Rev.* B **51** 13942
[22] Park J H, Cheong S W and Chen C T 1997 *Phys. Rev.* B **55** 11072
[23] Sarma D D, Shanthi N, Barman S R, Hamada N, Sawada H and Terakura K 1995 *Phys. Rev. Lett.* **75** 1126
[24] Yeh J J and Lindau I 1985 *At. Data Nucl. Data Tables* **32** 1